Cancer Research

Activation of Robo1 Signaling of Breast Cancer Cells by Slit2 from Stromal Fibroblast Restrains Tumorigenesis via Blocking PI3K/Akt/β-Catenin Pathway

Po-Hao Chang[1], Wendy W. Hwang-Verslues[2], Yi-Cheng Chang[2], Chun-Chin Chen[2], Michael Hsiao[2], Yung-Ming Jeng[3], King-Jen Chang[4,5], Eva Y.-H.P. Lee[6], Jin-Yuh Shew[1,2], and Wen-Hwa Lee[6]

Abstract

Tumor microenvironment plays a critical role in regulating tumor progression by secreting factors that mediate cancer cell growth. Stromal fibroblasts can promote tumor growth through paracrine factors; however, restraint of malignant carcinoma progression by the microenvironment also has been observed. The mechanisms that underlie this paradox remain unknown. Here, we report that the tumorigenic potential of breast cancer cells is determined by an interaction between the Robo1 receptor and its ligand Slit2, which is secreted by stromal fibroblasts. The presence of an active Slit2/Robo1 signal blocks the translocation of β-catenin into nucleus, leading to downregulation of c-myc and cyclin D1 via the phosphoinositide 3-kinase (PI3K)/Akt pathway. Clinically, high Robo1 expression in the breast cancer cells correlates with increased survival in patients with breast cancer, and low Slit2 expression in the stromal fibroblasts is associated with lymph node metastasis. Together, our findings explain how a specific tumor microenvironment can restrain a given type of cancer cell from progression and show that both stromal fibroblasts and tumor cell heterogeneity affect breast cancer outcomes. *Cancer Res; 72(18); 4652–61. ©2012 AACR.*

Introduction

The development of mammary gland requires interplay of multiple cell types including luminal, epithelial, and myoepithelial cells, as well as stromal cells composed of fibroblasts, endothelial cells, adipocytes, and immune cells. Previous studies have shown that surrounding stroma is essential for normal mammary gland development such as proliferation, differentiation, and branching (1, 2). For example, amphiregulin-producing epithelial cells elicit paracrine activation of EGFR in stromal cells to dictate mammary ductal morphogenesis (3), and TGF-β mediates inhibition of mammary ductal and alveolar growth via epithelial-stromal interaction (4).

Stromal cells also play a critical role in tumor initiation and progression (5). Especially, stromal fibroblasts have a predominant role in cancer progression (6, 7). It is well established that tumor-associated stromal fibroblasts secrete high levels of hepatocyte growth factor (HGF) and stromal cell-derived factor-1 (SDF-1) to stimulate cancer cell growth through its receptors c-Met and CXCR4, respectively (8–10). TGF-β and metalloproteinase are also released from fibroblasts to promote tumorigenesis, regardless the normal function of TGF-β in inhibiting mammary gland growth (11, 12). Although most studies show that stromal cells positively regulate cancer growth, it has been observed that the microenvironment can restrain malignant progression of carcinoma (13, 14). For instance, small, early-stage carcinomas have been found in random autopsy sections of prostate tissues from subjects who died of causes unrelated to cancer (15). Such observations suggest that restrained growth of cancer cells is clinically prevalent. However, the mechanisms underlying these observations remain to be elucidated. Here, we showed that expression of Robo1 receptor in breast cancer cells coupling with Slit2 ligand secreted from stromal fibroblasts led to inhibition of tumor progression. These results explain, in part, how a specific microenvironment can restrain a given kind of cancer cell from further progression.

Materials and Methods

Ethics statement

Human breast cancer specimens and normal tissues were collected from National Taiwan University Hospital. All specimens were encoded to protect patients under protocols approved by the Institutional Review Board of Human Subjects

Authors' Affiliations: [1]Institute of Biochemistry and Molecular Biology, College of Medicine, National Taiwan University; [2]Genomics Research Center, Academia Sinica; [3]Department of Pathology and [4]Department of Surgery, National Taiwan University Hospital, Taipei; [5]Cheng Chin General Hospital, Taichung, Taiwan; and [6]Department of Biological Chemistry, University of California, Irvine, California

Note: Supplementary data for this article are available at Cancer Research Online (http://cancerres.aacrjournals.org/).

Corresponding Authors: Wen-Hwa Lee, Department of Biological Chemistry, University of California, Irvine, 124 Sprague Hall, Irvine, CA 92697-4037. Phone: 949-824-9766; Fax: 949-824-9767; E-mail: whlee@uci.edu; and J-Y Shew, Genomics Research Center, Academia Sinica, Taipei, Taiwan. E-mail: jyshew@gate.sinica.edu.tw

doi: 10.1158/0008-5472.CAN-12-0877

Research Ethics Committee of Academia Sinica and National Taiwan University, Taipei, Taiwan.

Cell lines and primary fibroblast isolation

Human breast cancer cell lines BT20, HCC1937, MDA-MB-157, MDA-MB-231, MDA-MB-361, MDA-MB-468, Hs578T, and SKBR3 were obtained from the American Type Culture Collection and maintained in Dulbecco's Modified Eagle Medium (DMEM) or DMEM/F12 supplemented with 10% FBS and antibiotics. Tumor tissues from patients were cut and digested with trypsin (9). Tissues were cultured until fibroblast grew and attached in petri dish. Primary fibroblasts were maintained in DMEM/F12 supplemented with 10% FBS.

Gene expression using microarray analysis, quantitative real-time PCR and immunoblotting

Total RNAs were extracted from breast cancer cell lines and fibroblasts with TRI reagent (Ambion). All cDNA were reversely transcribed with Superscript II transcriptase (Invitrogen). Affymetrix U133 Plus 2.0 human oligonucleotide microarrays were used to detect gene expression in MDA-MB-231, MDA-MB-361, Hs578T, and SKBR3 cells. Quantitative real-time PCR (qRT-PCR) was conducted using ABI Step-One SYBR-Green system (Applied Biosystems) according to the manufacturer's instruction and primers sequences are listed in Supplementary Table S1. For immunoblotting, whole-cell lysate was obtained using radioimmunoprecipitation assay lysis buffer. Nuclear and cytoplasmic proteins were extracted using ProteoJET Cytoplasmic and Nuclear Protein Extraction Kit (Thermo Scientific). The proteins were subjected to SDS-PAGE analysis followed by immunoblotting with various antibodies. Antibodies against β-catenin, α-tubulin, β-actin, p85, and Slit2 were purchased from GeneTex, Robo1, Robo2, and Robo4 from Abcam, histone deacetylases (HDAC) from Millpore, and phospho-Akt (Ser473) from Cell Signaling. Immobilon Western Chemiluminescent HRP Substrate (Millipore) was used to detect signals. NIH ImageJ was used for quantification.

Soft agar colony formation assay

Fifty thousand primary fibroblasts were seeded in a 12-well plate and cultured for 2 to 3 days to reach 60% to 70% confluence. After washing with PBS, a layer of DMEM/F12/FBS containing 0.5% agar was laid on top of the fibroblasts. A total of 2,500 breast cancer cells were seeded in a layer of 0.35% agar in DMEM/FBS over the bottom layer. After 14 to 21 days, crystal violet-stained colonies were counted. For experiments with addition of recombinant protein, 50 ng/mL of rSlit2 was added to the top layer every 3 days.

Lentivirus expression system

Short hairpin RNAs (shRNA) in pLKO-puro vectors were obtained from the National RNAi Core Facility, Taiwan. 293T cells were transfected with pMD.G, pCMVR8.91, and pLKO-puro-shRNA using lipofectamine 2000 (Invitrogen) for lentivirus packaging. For Robo1 overexpression, Lenti-X bicistronic lentiviral vector expression system (Clontech) was used according to the manufacture's instruction.

Mouse tumorigenicity assay

Animal experimental protocols were approved by the Institutional Animal Care and Utilization Committee, Academia Sinica. Nonobese diabetic/severe combined immunodeficiency (NOD/SCID) mice were implanted with 1×10^6 to 2×10^6 199Ct into fat pads a week before injection of 2×10^5 MDA-MB-231 or 5×10^5 HCC1937 cancer cells mixed with Matrigel (BD bioscience). Tumor volumes were measured every 4 to 5 days.

Immunohistochemistry

Formalin-fixed paraffin-embedded primary tumor tissue sections were used for immunohistochemistry (IHC). Heat-induced antigen retrieval was carried out using EDTA buffer (Trilogy) at 100°C. Endogenous peroxidase was eliminated with 3% H_2O_2. Slides were blocked in PBS containing 10% FBS and then incubated with primary antibodies against Slit2 and β-catenin overnight at 4°C. After washing, the slides were incubated with horseradish peroxidase rabbit/mouse polymer before visualization with liquid diaminobenzidine tetrahydrochloride plus substrate DAB chromogen from Dako REAL EnVision. All slides were counterstained with hematoxylin. For Robo1 staining, rabbit anti-goat IgG Alkaline Phosphatase (Southern Biotech) and NBT/BCIP were used for visualization. Robo1 expression was scored as "high" when more than 50% tumor cells were positive for membrane staining and "low" otherwise.

Coimmunoprecipitation assay

Robo1 overexpressing BT20 cells were serum starved for 6 hours and treated with rSlit2 for 10, 20, and 30 minutes. Cells were lysed and incubated in lysis buffer (150 mmol/L NaCl, 10 mmol/L Tris pH 7.5, 2 mmol/L Mg_2Cl_2, and 1% Triton X-100) for 30 minutes at 4°C. Cell lysates were precleaned with normal mouse/rabbit IgG and A/G beads (Santa Cruz) for 2 hours at 4°C. Immunoprecipitation was carried out using antibodies against Robo1, p85, and mouse/rabbit IgG overnight at 4°C. The antigen–antibody complex was immobilized with A/G beads for 2 hours at 4°C. After washed with wash buffer (150 mmol/L NaCl, 10 mmol/L Tris pH 7.5, 2 mmol/L Mg_2Cl_2, and 0.1% Triton X-100), proteins were eluted by addition of loading dye and boiling at 95°C for 2 minutes. The proteins were subjected to SDS-PAGE analysis followed by immunoblotting with various antibodies.

Immunofluorescence

Control and shRobo1 of MDA-MB-231 cells were seeded on coverslips and treated with rSlit2. The cells were washed with PBS, fixed in 4% paraformaldehyde for 10 minutes, washed with PBS and permeabilized in 0.2% Triton X-100 for 15 minutes. After washed with PBS, cells were blocked with PBS containing 10% FBS for 2 hours before incubation with the primary antibody as indicated anti-β-catenin overnight at 4°C. The cells were incubated for 1 hour with a fluorochrome-conjugated secondary antibody (Alexa Fluor 488 anti-mouse). Coverslips with stained cells were then washed with PBS, stained with 4′,6-diamidino-2-phenylindole (DAPI), and mounted onto glass slides with Vectashield Mounting Medium (Vector Laboratories). For the primary tumor tissue sections, 100°C EDTA

buffer was used for heat-induced antigen retrieval. Slides were blocked in PBS containing 10% FBS and then incubated with primary antibodies against Slit2 (Sigma) and α-smooth muscle actin (α-SMA; Dako) overnight at 4°C. The slides were incubated for 1 hour with fluorochrome-conjugated secondary antibody (Alexa Fluor 488 anti-mouse or Alexa Fluor 594 anti-rabbit). Slides were then stained with DAPI and mounted onto glass slides with mounting medium.

Statistical methods

For soft agar colony formation and tumorigenicity assay, all data were presented as means ± SD, and Student *t* test was used to compare control and treatment groups. Asterisk (*) indicated statistical significance with *P* value less than 0.05. Asterisks (**) indicated statistical significance with *P* less than 0.01. The association between Robo1 gene expression and survival of patients with breast cancer was estimated using univariate Cox proportional-hazards regression analysis, whereas the association among survival, Robo1 gene expression and other clinical predictors including age, tumor size, distant metastasis, lymph node status, tumor grade, estrogen receptor expression, and Her2/neu expression was analyzed by multivariate Cox regression analysis. HR was evaluated using the method of Grambsch and Therneau. No violation of the proportional assumption was detected. The optimal cutoff point of Robo1 gene expression for 5-year survival was determined by receiver operating characteristic curve (ROC) analysis. The survival curve and the statistics were generated by Kaplan–Meier method and log-rank test, respectively (16). The correlation between Slit2 gene expression and lymph node metastasis after adjustment for other clinical predictors was estimated using partial Pearson's correlation.

Results

Stromal fibroblasts can either suppress or promote tumorigenicity of breast cancer cells

Initially, we determined how stromal fibroblasts affect breast cancer cell tumorigenic activity by conducting a series of soft

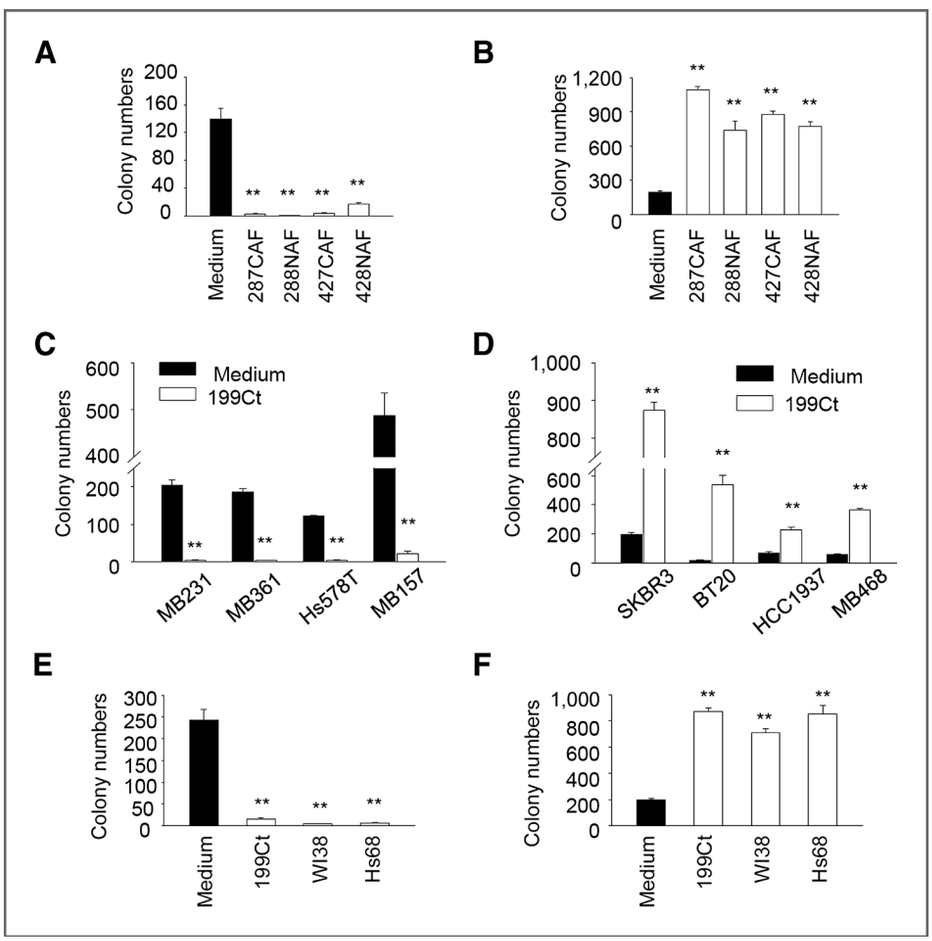

Figure 1. Stromal fibroblasts can either promote or suppress soft agar colony formation of breast cancer cells. A and B, soft agar colony formation assays using MDA-MB-231 (A) and SKBR3 (B) cells cocultured with primary CAF or normal breast-associated fibroblasts (NAF). C and D, soft agar colony formation assays using breast cancer cell lines other than MDA-MB-231 and SKBR3 cocultured with immortalized human CAF (199Ct). Colony formation in MDA-MB-361, Hs578T, and MDA-MB-157 cells was inhibited (C), but increased in HCC1937, BT20, and MDA-MB-468 cells (D) when cocultured with 199Ct. E and F, soft agar colony formation assays using MDA-MB231 (E) and SKBR3 (F) cells cocultured with 2 other human fibroblast cell lines, WI38 and Hs68. All data points were carried out in triplicates and all experiments were carried out at least 3 times with similar results. Data show means ± SD. **, $P < 0.01$.

agar colony formation assays using a bottom agar layer containing fibroblasts and an upper agar layer containing breast cancer cells (hereafter referred to as coculture). MDA-MB-231 and SKBR3 were cocultured with primary fibroblasts (carcinoma-associated fibroblasts, CAF; normal breast-associated fibroblasts, NAF) isolated from patients with breast cancer. Surprisingly, 2 opposite phenotypes were observed that stromal fibroblasts suppressed colony formation in MDA-MB-231 cells but promoted it in SKBR3 (Fig. 1A and B). Suppression was also observed in additional breast cancer cell lines including MDA-MB-361, Hs578T, and MDA-MB-157 (Fig. 1C), whereas promotion was observed in BT20, HCC1937, and MDA-MB-468 cell lines (Fig. 1D). Furthermore, these opposite phenotypes were also observed when cancer cells were cocultured with immortalized human CAFs (199Ct) and human fibroblast cell lines (WI38 and Hs68). The colony formation of MDA-MB-231 was reduced (Fig. 1E), but increased in SKBR3 (Fig. 1F). These results suggested that fibroblasts could either promote or suppress tumorigenic activity of different breast cancer cells.

Identification of Robo1 as a candidate receptor for fibroblast-associated tumor suppression

The design of the coculture system strongly suggested that the suppression mechanism is most likely to be mediated by signaling through soluble factors secreted by fibroblasts to the receptors on breast cancer cells. To identify potential receptor, we used human cDNA microarrays to compare the mRNA expression profiles among MDA-MB-231, MDA-MB-361, Hs578T, and SKBR3 cells (Fig. 2A). Of the 610 genes that are upregulated in MDA-MB-231, MDA-MB-361, and Hs578T cells compared with SKBR3 cells, 8 encoded receptors (Fig. 2B). qRT-PCR analysis confirmed the expression profiles of these 8 receptors to be similar to that of the cDNA microarrays (Fig. 2C). Within these 8 candidate receptors, Robo1 had an expression profile consistent with the contrasting phenotypes of the fibroblast-suppressed cell lines MDA-MB-231, MDA-MB-361, and MDA-MB-157 (high Robo1 expression) versus the fibroblast-promoted cancer cell lines BT20, HCC1937, and SKBR3 (low Robo1 expression). Because there are multiple Robo

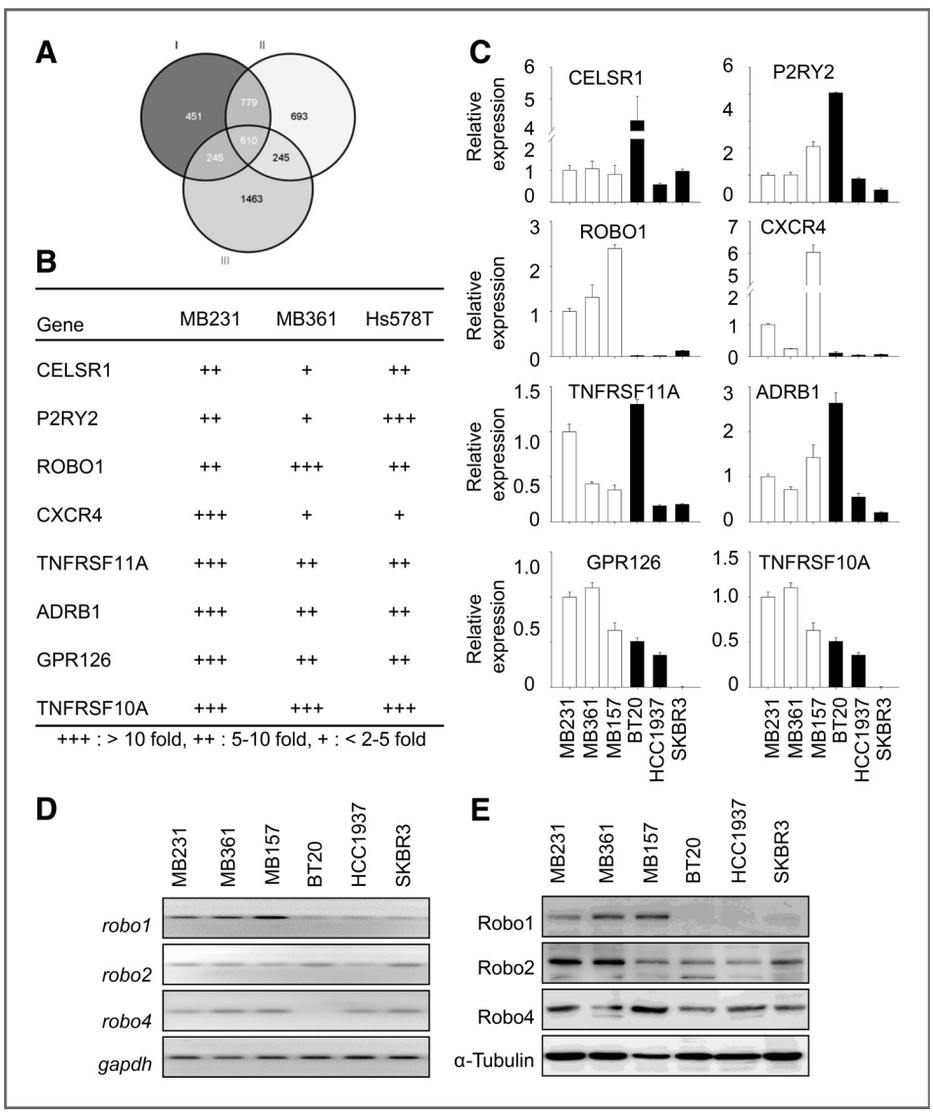

Figure 2. Robo1 is identified as a candidate receptor involved in fibroblast-mediated tumor suppression. A, summary of cDNA microarray analyses. Total 610 genes expressed at least 2-fold higher in MDA-MB-231 (I), MDA-MD-361 (II), and Hs578T (III) than in SKBR3 were found by Affymetrix microarray analysis. B, eight transmembrane receptors were identified among the 610 genes with their expression pattern matched with the profile that MDA-MB-231, MDA-MB-361, and Hs578T had a higher level than that of SKBR3. C, reconfirming the expression profile of the 8 transmembrane receptors in 6 different breast cancer cells. Their receptor mRNA expressions were measured directly by qRT-PCR with *Gapdh* as an internal control. D and E, mRNA and protein expressions of Robo1, 2, and 4 were measured by RT-PCR (D) and immunoblotting (E), respectively. *Gapdh* and α-tubulin served as loading controls for RNA and protein expression, respectively.

receptor members been reported to be involved in tumorigenesis (17, 18), we then examined the expressions of Robo1, Robo2, and Robo4 at both mRNA and protein levels among these breast cancer cell lines. It seemed that only Robo1 had high expression in MDA-MB-231, MDA-MB-361, and MDA-MB-157 but low in BT20, HCC1937, and SKBR3 cell lines, whereas Robo2 and Robo4 were ubiquitously expressed in all breast cancer cell lines tested (Fig. 2D and E), suggesting that Robo1 may be the differentially expressed receptor mediating fibroblast suppression in certain breast cancer cell lines.

Robo1 mediates fibroblast-associated tumor suppression

To directly test whether Robo1 plays such a role in fibroblast-mediated suppression of breast tumorigenicity, we established 2 independent clones of MDA-MB-231 cells with Robo1 depleted using a lentivirus shRNA system (Fig. 3A). The colony formation of these 2 clones was greatly enhanced in fibroblast coculture assay compared with the parental control (Fig. 3B). Furthermore, coinjection of Robo1-depleted MDA-MB-231 cells with 199Ct into fat pads of NOD/SCID mice generated significantly larger tumors compared with the parental MDA-MB-231 control (Fig. 3C and Supplementary Fig. S1A). Identical results were also observed when MDA-MB-157 cells were used (Fig. 3D and E). Moreover, depletion of Robo2 had no effect on colony forming activity of MDA-MB-231 cells (Supplementary Fig. S2), confirming the differentially expressed Robo1 is the key player. Conversely, ectopic expression of Robo1 in BT20 and HCC1937 cells (Fig. 3F), which had low endogenous Robo1 expressions and failed to suppress colony-forming abilities, resulted in a significant decrease in colony formation (Fig. 3G). Consistently, coinjection of HCC1937 cells expressing Robo1 with fibroblasts into NOD/SCID mice fat pads generated much smaller tumors compared with the parental HCC1937 cells (Fig. 3H and Supplementary Fig. S1B). Taken together, these results indicated that the presence of Robo1 in cancer cells plays a critical role in fibroblast-mediated suppression of tumorigenesis.

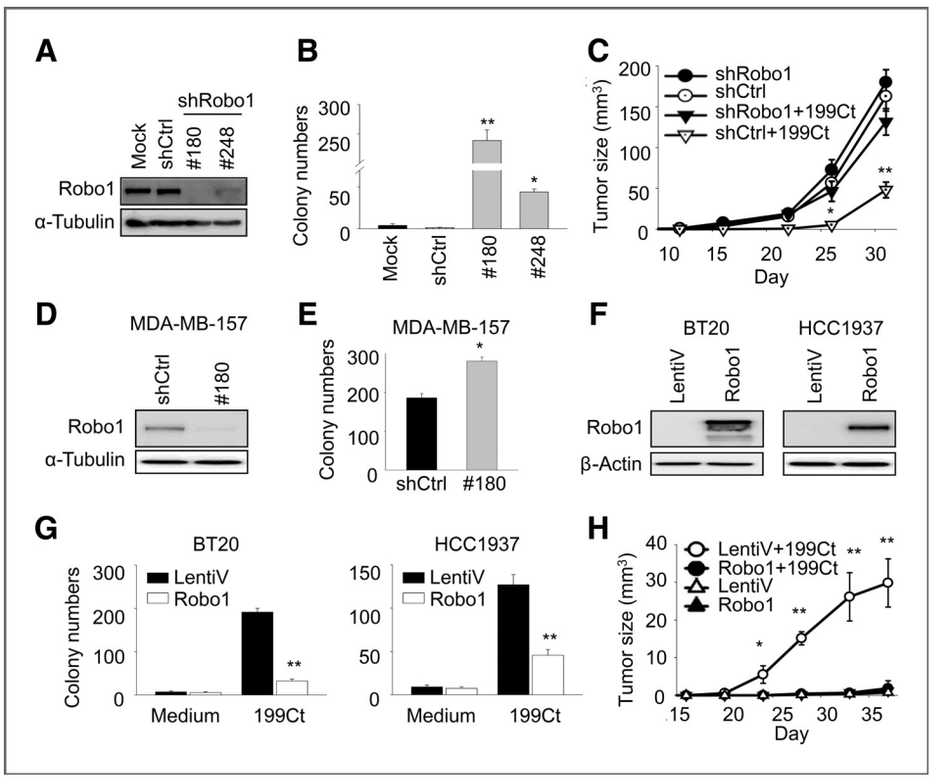

Figure 3. Robo1 plays an essential role in fibroblast-mediated suppression of breast tumorigenesis. A, immunoblotting analysis of Robo1 expression in MDA-MB-231 cells infected by 2 independent lentiviruses, #180 and #248, carrying shRobo1. Cells infected with lentiviral sh-luciferease (shCtrl) or uninfected (Mock) served as controls. α-Tubulin was used as a loading control. B, soft agar colony formation assays using Mock, shCtrl, and shRobo1 MDA-MB-231 cells cocultured with 199Ct. C, tumor growth assay in NOD/SCID mice. shCtrl or shRobo1 MDA-MB-231 cells were injected into mammary fat-pad with or without 199Ct and the tumor volumes were measured every 4 to 5 days. D, immunoblotting analysis of Robo1 expression in MDA-MB-157 cells infected by shRobo1 #180. Cells infected with shCtrl served as the control. α-Tubulin was used as a loading control. E, soft-agar colony formation assays using shCtrl and shRobo1 MDA-MB-157 cells cocultured with 199Ct. F, immunoblotting analysis of ectopic expression of Robo1 in BT20 and HCC1937 cells. Cells were infected either with lentiviruses carrying Robo1 cDNA (Robo1) or empty vector (LentiV). β-Actin was used as a loading control. G, soft agar colony formation assay for LentiV and Robo1 overexpressing BT20 and HCC1937 cells cocultured with or without 199Ct. H, tumor growth assay in NOD/SCID mice. HCC1937 cells expressing Robo1 or control (LentiV) were injected into mammary fat-pad with or without 199Ct and the tumor volumes were measured every 4 to 5 days. All data points were carried out in triplicates and all *in vitro* experiments were carried out at least 3 times. Data show means ± SD. For tumor growth assay in NOD/SCID mice, 6 mice per group were used. *, $P < 0.05$; **, $P < 0.01$.

Slit2 secreted from stromal fibroblasts inhibits tumorigenesis via Robo1 receptor

It has been reported that Slit2 serves as a Robo1 ligand in central nervous system to exhibit midline repellent (19, 20). Expression of Slit2 from fibroblasts may be responsible for the Robo1 suppression of tumorigenesis. We first examined Slit2 expression in breast cancer cell lines (MDA-MB-231, MDA-MB-361, SKBR3, and BT20), fibroblast cell lines (199Ct, WI38, and HS68), and primary fibroblasts (221C, 222N, 288N, and 428N). We found that Slit2 level was 4- to 15-fold higher in fibroblasts than in MDA-MB-231 cells, which expressed the highest level of Slit2 among the breast cancer cell lines (Fig. 4A). Consistently, immunostaining analysis of primary cancer specimens showed that Slit2 expression was higher in stromal fibroblasts than in tumor cells (Fig. 4B and Supplementary Fig. S3). To test the potential role of secreted Slit2 in tumorigenesis, we added conditioned medium harvested from Slit2-expressing 199Ct to MDA-MB-231 cells cultured in soft agar. Addition of conditioned medium can reduce colony formation in a dose-dependent manner (Fig. 4C). In contrast, coculture with Slit2-depleted 199Ct cells did not inhibit colony formation of MDA-MB-231 (Fig. 4D and E). Furthermore, when purified recombinant Slit2 protein (rSlit2) was added to MDA-MB-231 cells, the colony numbers of MDA-MB-231 cells decreased about 60%, whereas the Robo1-depleted cells showed no response to rSlit2 (Fig. 4F). Together, these results showed that Slit2 secreted from fibroblasts suppresses tumor growth via Robo1 receptor.

Slit2/Robo1 signaling blocks nuclear translocation of β-catenin via PI3K/Akt pathway

Slit2/Robo1 signaling has been associated with decreasing Akt phosphorylation and downregulation of β-catenin activity (21, 22). Moreover, phosphoinositide 3-kinase (PI3K)/Akt/β-catenin signaling is highly activated in breast cancers (23, 24). Slit2 secreted from the surrounding fibroblasts may suppress tumorigenic ability of cancer cells by inhibiting the PI3K/Akt/β-catenin pathway through Robo1 receptor. To examine this possibility, we carried out co-immunoprecipitation (Co-IP) assay with anti-Robo1 antibody and found that Robo1 was immunoprecipitated with p85, a subunit of PI3K, within 10 to 30 minutes upon rSlit2 treatment (Fig. 5A). Reciprocal Co-IP with anti-p85 antibody further confirmed the Robo1–p85 interaction (Supplementary Fig. S4). The phospho-Akt activity was also decreased in rSlit2-treated control cells, but not the Robo1-depleted cells (Fig. 5B, lanes 1 vs. 2 and lanes 3 vs. 4, respectively). Consistently, using cellular fractionation and immunoblotting, we found that the amount of nuclear β-catenin was reduced in the control cells but not the Robo1-depleted cells when cocultured with 199Ct (Fig. 5C, lanes 7 and 8), although the β-catenin expression levels were comparable between the control and Robo1-depleted cells (Supplementary Fig. S5). Supportively, upon rSlit2 treatment, an enhanced nuclear localization of β-catenin in the Robo1-depleted cells was detected by immunofluorescence assay (Fig. 5D), whereas the expression of cyclin D1 or c-myc in cells expressing Robo1 was reduced about 2-folds (Fig. 5E). Conforming to these findings, reduction of nuclear β-catenin was observed in tumor specimens with either high Robo1

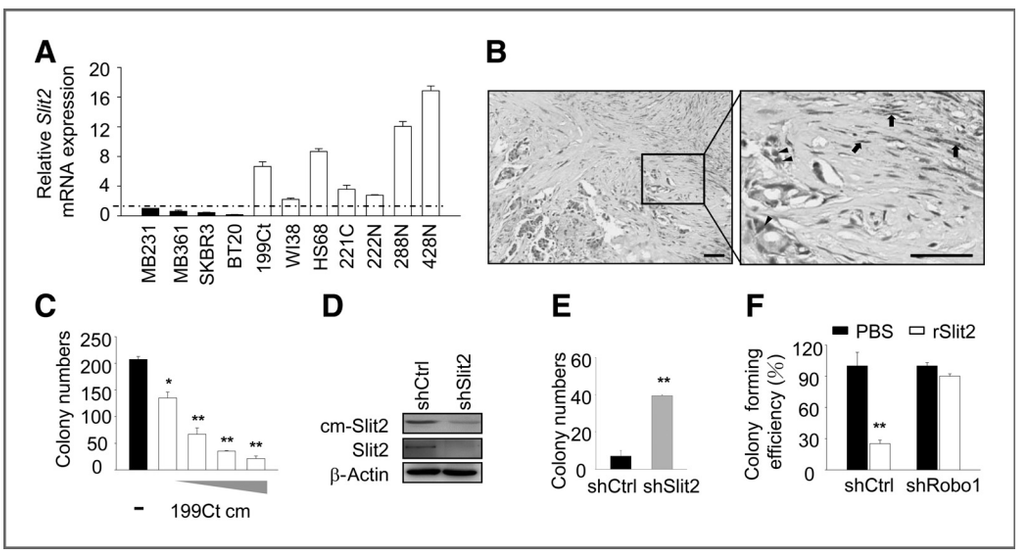

Figure 4. Slit2 secreted from stromal fibroblasts inhibits cancer cell tumorigenesis. A, *Slit2* mRNA expression in breast cancer cell lines (MDA-MB-231, MDA-MB-361, SKBR3, and BT20), fibroblast cell lines (199Ct, WI38, and HS68), and primary fibroblasts (221C, 222N, 288N, and 428N) was examined by qRT-PCR. B, IHC staining with antibody against Slit2 in breast cancer specimen. Low magnification (left); scale bar, 25 μm. High-magnification (right); scale bar, 50 μm. Arrows indicate stromal fibroblasts. Arrowheads indicate cancer cells. C, soft-agar colony formation assay for MDA-MB-231 cells treated with conditioned medium (199Ct cm) collected from 199Ct culture. D, immunoblotting analysis of Slit2 proteins in harvested conditioned medium (cm-Slit2) from shCtrl or shSlit2 199Ct. β-Actin was used as a loading control. E, soft agar colony formation assay for MDA-MB-231 cells cocultured with shCtrl or shSlit2 199Ct. F, soft agar colony formation of shCtrl and shRobo1 MDA-MB-231 cells treated with PBS or 50 ng/mL of recombinant Slit2 (rSlit2) protein. All data points were carried out in triplicates and all experiments were carried out at least 3 times. Data show means ± SD. *, $P < 0.05$; **, $P < 0.01$.

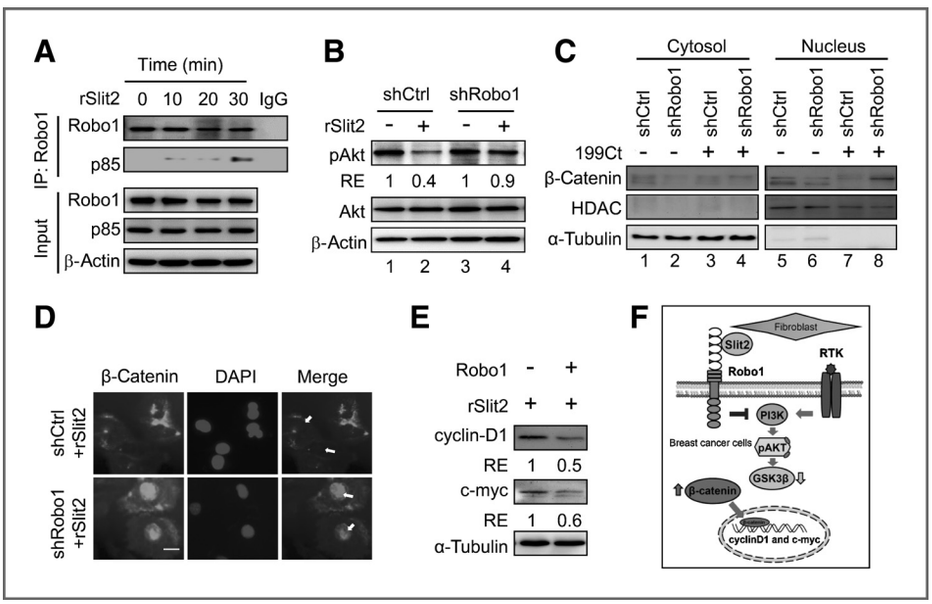

Figure 5. Slit2/Robo1 signaling blocks β-catenin translocation through PI3K/Akt pathway. A, Robo1 overexpressing BT20 cells were treated with rSlit2 (200 ng/mL) for 10, 20, and 30 minutes. Coimmunoprecipitation of Robo1 and p85 was detected using immunoblotting analysis in response to the rSlit2 treatment. Normal IgG (IgG) was used as a negative coimmunoprecipitation control. β-Actin served as a loading control. B, immunoblotting analysis of phospho-Akt in shCtrl and shRobo1 MDA-MB-231 cells treated with rSlit2 (200 ng/mL). Total Akt was used as a quantification control. β-Actin served as a loading control. Relative expression (RE) in phospho-Akt to total Akt protein levels is indicated. C, immunoblotting assay of β-catenin in cytosolic and nuclear fractions of the shCtrl and shRobo1 MDA-MB-231 cells cocultured with or without 199Ct. α-Tubulin and HDAC were used as cytosolic and nuclear markers, respectively. D, immunofluorescence staining with antibody against β-catenin for shCtrl and shRobo1 MDA-MB-231 cells after treatment with rSlit2 (200 ng/mL). Scale bar, 20 μm. Arrows indicate nuclei. E, immunoblotting analysis of shCtrl and shRobo1 MDA-MB-231 cells treated with rSlit2 using antibodies against cyclin D1 and c-myc. α-Tubulin as a loading control. RE in cyclin D1 and c-myc to α-tubulin protein levels is indicated. F, diagram summarizes the pathway of how Slit2/Robo1 signal is transmitted from stromal fibroblasts to breast cancer cells.

expression in cancer cells or high Slit2 expression in stromal fibroblast (Supplementary Fig. S6). Together, these results suggested that activation of Slit2/Robo1 signaling inhibits the PI3K/Akt pathway to block β-catenin nuclear translocation and downregulate cyclin D1 and c-myc expression (Fig. 5F).

High expression of either Robo1 in breast cancer cells or Slit2 in stromal fibroblasts is associated with better breast cancer prognosis

The above results imply that the Slit2/Robo1 pathway plays an essential role in fibroblast-mediated tumor suppression. We then analyzed the expression levels of Robo1/Slit2 in 3 cohorts of breast cancer patient specimens (Supplementary Table S2–S5). The expression of Robo1 mRNA measured by qRT-PCR in breast cancer tissues was positively correlated with survival of patients with breast cancer ($P = 0.006$, Table 1) in the first cohort (characteristics of patients were provided in Supplementary Table S2). The correlation remained significant after adjustment for age, tumor size, distant metastasis, lymph node involvement, estrogen–receptor expression, and Her2/neu gene expression ($P = 0.02$, Table 1). Furthermore, patients with high Robo1 mRNA expression showed better prognosis

Table 1. Univariate and multivariate proportional hazards analysis of mortality of patients with breast cancer

	Univariate		Multivariate	
Variables	**HR (95% CI)**	***P***	**HR (95% CI)**	***P***
Robo1 gene expression (per 2-fold increase)	0.81 (0.71–0.94)	0.006	0.84 (0.74–0.98)	0.02
Age (per decade)	0.99 (0.97–1.01)	0.52	1.00 (0.97–1.03)	0.63
Tumor size (per grade)	1.63 (1.24–2.26)	0.0008	1.33 (0.90–1.95)	0.14
Distant metastasis	4.04 (1.44–11.27)	0.007	5.25 (1.01–27.13)	0.04
Lymph node positivity	3.56 (2.21–5.72)	<0.0001	3.40 (1.84–6.26)	<0.001
Estrogen–receptor expression (per point)	0.71 (0.54–0.96)	0.02	0.48 (0.32–0.72)	0.0005
Her2/neu gene expression (per point)	1.15 (0.69–1.90)	0.60	1.54 (0.79–2.98)	0.19

Abbreviations: HR, hazard ratio; CI, confidence interval.

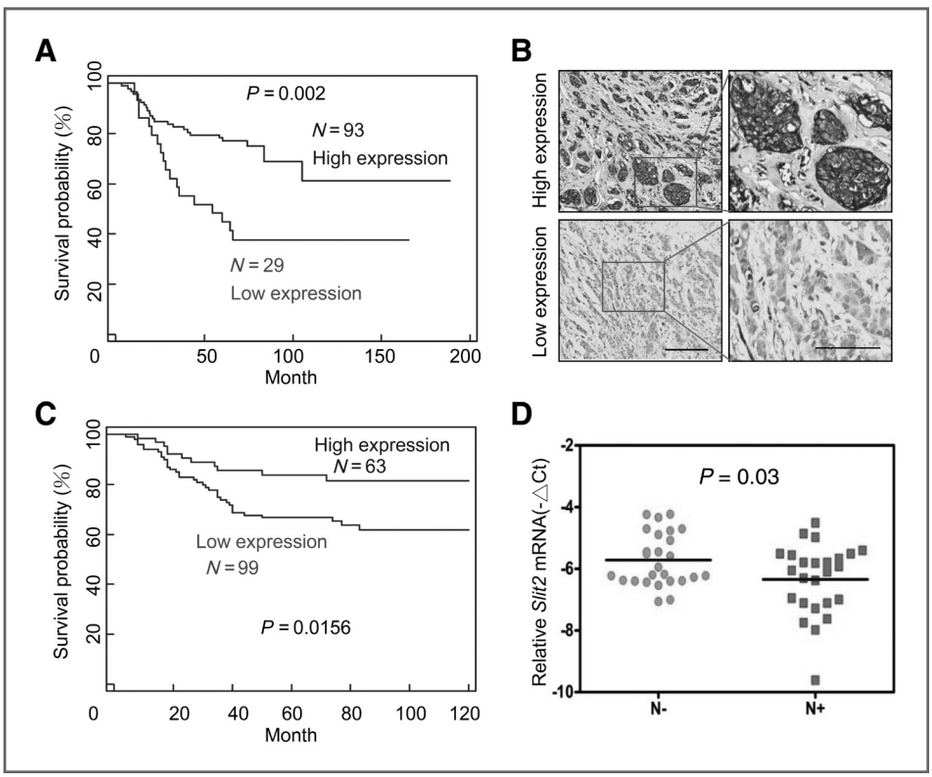

Figure 6. Clinical relevance of Robo1/Slit2 expression in breast cancer specimens. A, Kaplan–Meier survival analysis for 122 patients with breast cancer divided into 2 groups on the basis of their Robo1 mRNA expression levels. B, IHC staining of Robo1 in breast tumor specimens. Low-magnification (left); scale bar, 100 μm. High magnification (right); scale bar, 50 μm. C, Kaplan–Meier survival analysis for 162 breast cancer specimens using IHC staining to detect Robo1 expression in cancer cell membrane. D, fifty-one CAFs isolated from freshly obtained specimens were used to determine the correlation between *Slit2* mRNA expression and metastasis status of the patients. *Slit2* mRNA levels were measured by qRT-PCR and compared with the internal control gene *Gapdh*. Patients were divided into 2 groups according to the metastasis status to correlate with the relative *Slit2* mRNA expression. N−, no lymph node metastasis ($n = 26$); N+, with lymph node metastasis ($n = 25$).

than those with low Robo1 expression (log-rank $P = 0.002$, Fig. 6A) when those patients were grouped on the basis of a cutoff value determined by ROC analysis (25). Consistently, patients with high Robo1 protein expression determined by IHC (Fig. 6B) had positively correlation with survival of patients with breast cancer ($P = 0.019$, Supplementary Table S3) in the second cohort (characteristics of patients were provided in Supplementary Table S4). The correlation remained significant after adjustment for age, tumor size, distant metastasis, lymph node involvement, estrogen–receptor expression, and Her2/neu gene expression ($P = 0.02$, Supplementary Table S3). Patients with high Robo1 protein expression showed better prognosis than those with low Robo1 protein expression (log-rank $P = 0.0156$, Fig. 6C). Supportively, a cDNA microarray analysis revealed that low Slit2 expression in stromal cells correlated with poor outcome in breast cancer (26). Consistent with this observation, high Slit2 mRNA expression in stromal fibroblasts was correlated with low frequency of lymph node metastasis in the third cohort (characteristics of patients were provided in Supplementary Table S5) of freshly obtained samples ($P = 0.03$, Fig 6D). The correlation remained significant after adjustment for age, tumor size, and estrogen–receptor expression ($P = 0.04$). Taken together, these results further suggested that high expression of either Robo1 in breast cancer cells or Slit2 in stromal fibroblasts is associated with better prognosis in breast cancer.

Discussion

Cancer originates from genetic alterations in progenitor cells and progresses with constant modulation from its microenvironment composed of fibroblasts, endothelial cells, and immune cells (27). In this communication, we found that stromal fibroblasts enhanced tumorigenic activity of some breast cancer cells including BT20, HCC1937, and SKBR3, whereas suppressed others including MDA-MB231, MDA-MB361, and Hs578T (Fig. 1). The latter cancer cell group expressed Robo1 receptor, which recognizes ligand, Slit2, predominantly secreted from stromal fibroblasts (Fig 4). The presence of an active Slit2/Robo1 signaling inhibited the PI3K pathway by interacting with its subunit, p85, which led to inhibition of Akt phosphorylation, β-catenin translocation, and c-myc and cyclin D1 expression (Fig. 5). These results explain, in part, how specific stromal fibroblasts expressing Slit2 can restrain a given kind of cancer cell expressing Robo1 from progression.

Slit2 and Robo1 were first identified in the development of central nervous system (28). Interestingly, Slit2/Robo1 signaling plays a role in regulating outgrowth of mammary branches

by inhibiting nuclear translocation of β-catenin in the basal myoepithelial cells (21), suggesting the regulatory role of Slit2/Robo1 in mammary gland development. Loss of either Slit2 from fibroblasts or Robo1 from epithelial progenitor cells disrupts the normal development of mammary gland. Homozygous deletion and promoter methylation of Robo1 have been observed in breast and lung cancer implicating a potential tumor suppressor role of Robo1 (29, 30). A recent study reported that endothelial cell-secreted Slit2 suppresses tumor growth and motility in mouse mammary adenocarcinoma (31). Moreover, our clinical data showed that patients with breast cancer and low Robo1 expression in the cancer cells have worse prognosis (Fig. 6). Consistent with these findings, we suggested that regulation of Slit2 in surrounding cells and Robo1 in cancer cells are important for cancer progression. Interestingly, upregulation of Robo1 has been reported to be correlated with poor prognosis in nasopharyngeal cancer (NPC; ref. 32). Although the precise mechanism to explain this apparent discrepancy remains unclear, it is likely that Robo1 may have other distinctive function in NPC or the microenvironment of NPC is substantially different from that of breast cancer.

Activation of the PI3K/Akt signaling pathway results in aberrant cell proliferation, tumorigenesis and metastatic competence (33). In many types of human cancer, Akt mediated β-catenin nuclear accumulation and increased transcriptional activity that promotes tumor development (34). Our observation showed that activation of Slit2/Robo1 suppresses Akt phosphorylation and indirectly blocks β-catenin translocation from cytoplasm to nucleus. Furthermore, we also showed that β-catenin accumulates in membrane instead of nucleus in patients with breast cancer and high Robo1 and Slit2 expression, supporting the importance of the Slit2/Robo1-mediated suppression of Akt/β-catenin activity in breast tumorigenesis. It has been shown that the Slit2/Robo1 signal serves as an inhibitory cue to block β-catenin activity (22, 35). Consistent with these reports, fibroblast-secreted Slit2 blocked β-catenin activity in tumorigenesis of Robo1 expressing cancer cells. It was noted that the Src homology (SH) domain of PI3K-associated p85 is critical for binding to tyrosine kinase receptors to activate downstream Akt signaling (36). Our observation that Robo1 bound to p85 and suppressed phosphorylation of Akt upon addition of Slit2 suggests a potential inhibitory effect for tyrosine kinase receptors. Whether Robo1/Slit2 signaling suppressing tumorigenesis acts on additional pathways remains to be further explored.

The restraint of cancer cells by fibroblasts has to be disrupted as cancer progresses. This disruption can occur in different steps of the signaling pathway mediated by Slit2/Robo1. In addition to downregulate Slit2 and Robo1 expression, amplification of c-myc and cyclin D1 has been seen in many breast cancers (37, 38). Also, constitutively activation of Akt and augmentation of β-catenin-TCF/LEF transcriptional activity by mutation have been frequently seen in cancer cells (39, 40). These oncogenic alterations along with other oncogenic signal transduction pathways could help cancer cells to overcome the Slit2/Robo1-mediated restraint.

Our data that high Robo1 expression in breast cancer cells correlated with better patient survival and low Slit2 expression in stromal fibroblasts associated with lymph node metastasis provide useful and novel prognosis markers for breast cancer. Besides the genetic alteration in cancer cells, epigenetic or genetic alterations in cancer-associated stromal cells seem to have significant roles in regulating cancer progression. Therefore, these findings offer potential therapeutic targets for inducing tumor dormancy on the basis of the observation that stromal fibroblasts can suppress tumorigenicity of cancer cells via Slit2/Robo1 pathway.

Disclosure of Potential Conflicts of Interest

W.-H. Lee declares that he serves as a member of Board of Directors of the biotech company, GeneTex. This arrangement has been reviewed and approved by UCI conflict of interest committee.

Authors' Contributions

Conception and design: Po-H. Chang, W. W. Hwang-Verslues, E. Lee, W.-H. Lee
Development of methodology: Po-H. Chang, W. W. Hwang-Verslues, J.-Y. Shew
Acquisition of data (provided animals, acquired and managed patients, provided facilities, etc.): Po-H. Chang, C.-C. Chen, M. Hsiao, Y.-M. Jeng, K.-J. Chang
Analysis and interpretation of data (e.g., statistical analysis, biostatistics, computational analysis): Po-H. Chang, Yi-C. Chang, M. Hsiao, Y.-M. Jeng, E. Lee, W.-H. Lee
Writing, review, and/or revision of the manuscript: Po-H. Chang, W. W. Hwang-Verslues, E. Lee, W.-H. Lee
Administrative, technical, or material support (i.e., reporting or organizing data, constructing databases): Po-H. Chang, J.-Y. Shew
Study supervision: Po-H. Chang, W. W. Hwang-Verslues, J.-Y. Shew, W.-H. Lee

Acknowledgments

The authors thank Emily Guo for critical reading of the manuscript.

Grant Support

This work was supported by Academia Sinica (Taiwan) and NIH grants to E. Lee (CA137102) and W.-H. Lee (CA94170). W. W. Hwang-Verslues was supported by an Academia Sinica Postdocotral Research Fellowship.

The costs of publication of this article were defrayed in part by the payment of page charges. This article must therefore be hereby marked *advertisement* in accordance with 18 U.S.C. Section 1734 solely to indicate this fact.

Received March 8, 2012; revised June 29, 2012; accepted July 15, 2012; published OnlineFirst July 23, 2012.

References

1. Wiseman BS, Werb Z. Stromal effects on mammary gland development and breast cancer. Science 2002;296:1046–9.
2. Polyak K, Kalluri R. The role of the microenvironment in mammary gland development and cancer. Cold Spring Harb Perspect Biol 2010;2:a003244.
3. Sternlicht MD, Sunnarborg SW, Kouros-Mehr H, Yu Y, Lee DC, Werb Z. Mammary ductal morphogenesis requires paracrine activation of stromal EGFR via ADAM17-dependent shedding of epithelial amphiregulin. Development 2005;132:3923–33.
4. Daniel CW, Robinson S, Silberstein GB. The role of TGF-beta in patterning and growth of the mammary ductal tree. J Mammary Gland Biol Neoplasia 1996;1:331–41.
5. Liotta LA, Kohn EC. The microenvironment of the tumour-host interface. Nature 2001;411:375–9.

6. Kalluri R, Zeisberg M. Fibroblasts in cancer. Nat Rev Cancer 2006;6:392–401.
7. Bhowmick NA, Neilson EG, Moses HL. Stromal fibroblasts in cancer initiation and progression. Nature 2004;432:332–7.
8. Rong S, Bodescot M, Blair D, Dunn J, Nakamura T, Mizuno K, et al. Tumorigenicity of the met proto-oncogene and the gene for hepatocyte growth factor. Mol Cell Biol 1992;12:5152–8.
9. Tyan SW, Kuo WH, Huang CK, Pan CC, Shew JY, Chang KJ, et al. Breast cancer cells induce cancer-associated fibroblasts to secrete hepatocyte growth factor to enhance breast tumorigenesis. PLoS One 2011;6:e15313.
10. Orimo A, Gupta PB, Sgroi DC, Arenzana-Seisdedos F, Delaunay T, Naeem R, et al. Stromal fibroblasts present in invasive human breast carcinomas promote tumor growth and angiogenesis through elevated SDF-1/CXCL12 secretion. Cell 2005;121:335–48.
11. Ma C, Rong Y, Radiloff DR, Datto MB, Centeno B, Bao S, et al. Extracellular matrix protein betaig-h3/TGFBI promotes metastasis of colon cancer by enhancing cell extravasation. Genes Dev 2008;22:308–21.
12. Littlepage LE, Sternlicht MD, Rougier N, Phillips J, Gallo E, Yu Y, et al. Matrix metalloproteinases contribute distinct roles in neuroendocrine prostate carcinogenesis, metastasis, and angiogenesis progression. Cancer Res 2010;70:2224–34.
13. Woodruff M. The Hubert, Walter Lecture, 1982—Interaction of Cancer and Host. Brit J Cancer 1982;46:313–22.
14. Bissell MJ, Hines WC. Why don't we get more cancer? A proposed role of the microenvironment in restraining cancer progression. Nat Med 2011;17:320–9.
15. Rich AR. On the frequency of occurrence of occult carcinoma of the prostrate. 1934. Int J Epidemiol 2007;36:274–7.
16. van de Vijver MJ, He YD, van't Veer LJ, Dai H, Hart AA, Voskuil DW, et al. A gene-expression signature as a predictor of survival in breast cancer. N Engl J Med 2002;347:1999–2009.
17. Jones CA, London NR, Chen H, Park KW, Sauvaget D, Stockton RA, et al. Robo4 stabilizes the vascular network by inhibiting pathologic angiogenesis and endothelial hyperpermeability. Nat Med 2008;14:448–53.
18. Ghosh S, Ghosh A, Maiti GP, Alam N, Roy A, Roychoudhury S, et al. Alterations of ROBO1/DUTT1 and ROBO2 loci in early dysplastic lesions of head and neck: clinical and prognostic implications. Hum Genet 2009;125:189–98.
19. Brose K, Bland KS, Wang KH, Arnott D, Henzel W, Goodman CS, et al. Slit proteins bind Robo receptors and have an evolutionarily conserved role in repulsive axon guidance. Cell 1999;96:795–806.
20. Kidd T, Bland KS, Goodman CS. Slit is the midline repellent for the robo receptor in Drosophila. Cell 1999;96:785–94.
21. Macias H, Moran A, Samara Y, Moreno M, Compton JE, Harburg G, et al. SLIT/ROBO1 signaling suppresses mammary branching morphogenesis by limiting basal cell number. Dev Cell 2011;20:827–40.
22. Tseng RC, Lee SH, Hsu HS, Chen BH, Tsai WC, Tzao C, et al. SLIT2 attenuation during lung cancer progression deregulates beta-catenin and E-cadherin and associates with poor prognosis. Cancer Res 2010;70:543–51.
23. Fry MJ. Phosphoinositide 3-kinase signalling in breast cancer: how big a role might it play? Breast Cancer Res 2001;3:304–12.
24. Sun M, Paciga JE, Feldman RI, Yuan Z, Coppola D, Lu YY, et al. Phosphatidylinositol-3-OH Kinase (PI3K)/AKT2, activated in breast cancer, regulates and is induced by estrogen receptor alpha (ERalpha) via interaction between ERalpha and PI3K. Cancer Res 2001;61:5985–91.
25. Moses LE, Shapiro D, Littenberg B. Combining independent studies of a diagnostic test into a summary ROC curve: data-analytic approaches and some additional considerations. Stat Med 1993;12:1293–316.
26. Finak G, Bertos N, Pepin F, Sadekova S, Souleimanova M, Zhao H, et al. Stromal gene expression predicts clinical outcome in breast cancer. Nat Med 2008;14:518–27.
27. Mueller MM, Fusenig NE. Friends or foes - bipolar effects of the tumour stroma in cancer. Nat Rev Cancer 2004;4:839–49.
28. Tessier-Lavigne M, Goodman CS. The molecular biology of axon guidance. Science 1996;274:1123–33.
29. Sundaresan V, Chung G, Heppell-Parton A, Xiong J, Grundy C, Roberts I, et al. Homozygous deletions at 3p12 in breast and lung cancer. Oncogene 1998;17:1723–9.
30. Dallol A, Forgacs E, Martinez A, Sekido Y, Walker R, Kishida T, et al. Tumour specific promoter region methylation of the human homologue of the Drosophila Roundabout gene DUTT1 (ROBO1) in human cancers. Oncogene 2002;21:3020–8.
31. Brantley-Sieders DM, Dunaway CM, Rao M, Short S, Hwang Y, Gao Y, et al. Angiocrine factors modulate tumor proliferation and motility through EphA2 repression of Slit2 tumor suppressor function in endothelium. Cancer Res 2011;71:976–87.
32. Alajez NM, Lenarduzzi M, Ito E, Hui AB, Shi W, Bruce J, et al. MiR-218 suppresses nasopharyngeal cancer progression through downregulation of survivin and the SLIT2-ROBO1 pathway. Cancer Res 2011;71:2381–91.
33. Cantley LC, Neel BG. New insights into tumor suppression: PTEN suppresses tumor formation by restraining the phosphoinositide 3-kinase/AKT pathway. Proc Natl Acad Sci U S A 1999;96:4240–5.
34. Satyamoorthy K, Li G, Vaidya B, Patel D, Herlyn M. Insulin-like growth factor-1 induces survival and growth of biologically early melanoma cells through both the mitogen-activated protein kinase and beta-catenin pathways. Cancer Res 2001;61:7318–24.
35. Prasad A, Paruchuri V, Preet A, Latif F, Ganju RK. Slit-2 induces a tumor-suppressive effect by regulating beta-catenin in breast cancer cells. J Biol Chem 2008;283:26624–33.
36. Hu P, Margolis B, Skolnik EY, Lammers R, Ullrich A, Schlessinger J. Interaction of phosphatidylinositol 3-kinase-associated p85 with epidermal growth factor and platelet-derived growth factor receptors. Mol Cell Biol 1992;12:981–90.
37. Kononen J, Bubendorf L, Kallioniemi A, Barlund M, Schraml P, Leighton S, et al. Tissue microarrays for high-throughput molecular profiling of tumor specimens. Nat Med 1998;4:844–7.
38. Barbareschi M, Pelosio P, Caffo O, Buttitta F, Pellegrini S, Barbazza R, et al. Cyclin-D1-gene amplification and expression in breast carcinoma: relation with clinicopathologic characteristics and with retinoblastoma gene product, p53 and p21WAF1 immunohistochemical expression. Int J Cancer 1997;74:171–4.
39. Sharma M, Chuang WW, Sun Z. Phosphatidylinositol 3-kinase/Akt stimulates androgen pathway through GSK3beta inhibition and nuclear beta-catenin accumulation. J Biol Chem 2002;277:30935–41.
40. Samowitz WS, Powers MD, Spirio LN, Nollet F, van Roy F, Slattery ML. Beta-catenin mutations are more frequent in small colorectal adenomas than in larger adenomas and invasive carcinomas. Cancer Res 1999;59:1442–4.